Trends in Biomaterials and Artificial Organs
www.biomaterials.org.in/tibao
ISSN 0971-1198
https://doi.org/10.5281/zenodo.16959373

Original Article

Gold Nano-ELISA Fabrication for Longitudinal Salivary MMP-9 Detection

K. Hema Shree, R. Gayathri*, Vishnu Priya Veeraraghavan, J. Selvaraj, Pratibha Ramani, Ramya Ramadoss, K. Nitya

Department of Anatomy, Saveetha Dental College and Hospitals, Saveetha Institute of Medical and Technical Science, Saveetha University, Velappanchavadi, Chennai 600077, India

Received: *4 March 2025*
Accepted: *22 April 2025*
Published online: *26 August 2025*

Keywords: *MMP-9 detection, gold nano-ELISA, nigella sativa, thymoquinone, molecular docking, molecular dynamics simulation, ADME analysis, anti-inflammatory, natural MMP-9 inhibitor, diclofenac sodium*

MMP-9 has been found using traditional enzyme-linked immunosorbent tests (ELISA), although these methods have a limited sensitivity. This study aims to develop a gold nano-ELISA-based detection system for MMP-9 and investigate *Nigella sativa* (thymoquinone) as a natural inhibitor of MMP-9, comparing its efficacy with diclofenac sodium, a standard anti-inflammatory drug. Salivary MMP-9 levels in OSCC patients were measured both before and after treatment using gold-based nanoparticle-enhanced ELISA (Nano-ELISA) technology. The cytotoxic & anti-inflammatory properties of *Nigella sativa* extracts were assessed in comparison to diclofenac sodium using the MTT cytotoxic assay and the protein denaturation assay. In contrast to diclofenac, the binding stability and inhibitory capability of *Nigella sativa* bioactive components with MMP-9 were evaluated using molecule docking evaluation, molecular dynamics (MD) simulations, and energy decomposition analysis. Utilizing the ADME (absorption, distribution, metabolism, & excretion) analysis, the pharmacokinetics and drug-likeness of *Nigella sativa* components were assessed. The gold nano-ELISA method displayed great specificity and sensitivity for detecting salivary MMP-9, exhibiting a significant drop in levels post-treatment, indicating the possibility of using as a non-invasive biomarker for OSCC progression & therapeutic monitoring. *Nigella sativa* exhibited superior cytotoxicity compared to diclofenac sodium, reducing OSCC cell viability more effectively. However, diclofenac showed stronger anti-inflammatory activity in the protein denaturation assay. Molecular docking analysis revealed that *Nigella sativa* had a stronger binding affinity (-8.5 kcal/mol) and a lower inhibition constant (Ki = 580 nM) than diclofenac (-7.2 kcal/mol, Ki = 5.3 μM). MD simulations confirmed greater stability for *Nigella sativa* within the MMP-9 active site, with lower RMSD (1.8 Å) and higher ligand interaction retention (85%) compared to diclofenac (68%). Energy decomposition analysis further reinforced stronger electrostatic and Van der Waals interactions for *Nigella sativa*, confirming its higher inhibitory potential. The ADME analysis indicated that Nigella sativa has better pharmacokinetics, with high gastrointestinal absorption and lower CYP450 inhibition, reducing potential drug interaction risks compared to diclofenac. A promising technique for early OSCC evaluation and treatment monitoring, this study shows that gold nano-ELISA offers an efficient, non-invasive method for MMP-9 detection.

Introduction

OSCC, or oral squamous cell carcinoma, is one of the most common cancers of the head and neck area, making up over 90% of all oral cancers. Its high rates of morbidity and mortality, with an estimated 5-year survival rate of below fifty percent in advanced cases, continue to make it a major global health problem [1, 2].

OSCC progresses primarily due to dysregulated cellular processes, such as unchecked invasion, metastasis, and proliferation. MMP-9, an enzyme that has been implicated in tumor invasion, angiogenesis, and the breakdown of extracellular matrix (ECM), is a crucial molecular actor in these processes [3]. MMP-9 has been often found to be elevated in OSCC patients, indicating that it may be a biomarker for the course and outcome of the disease. Given its function in tumor biology, MMP-9 level detection that is both sensitive and accurate may be a useful diagnostic & prognostic tool for the treatment of OSCC [4].

Current diagnostic approaches for OSCC primarily involve

* *Coresponding author*
E-mail address: *sangeethas.sdc@saveetha.com* *(Dr. Gayathri. R, PhD, Department of Biochemistry, Saveetha Dental College and Hospital, Saveetha Institute of Medical and Technical science (SIMATS), Saveetha University, No. 162, Poonamalle High Road, Velappanchavadi, Chennai 600077, India)*

histopathological analysis of tissue biopsies, which, although accurate, are highly invasive, time-consuming, and often impractical for frequent monitoring [5]. The need for a non-invasive, cost-effective, and reliable biomarker-based detection method is critical for early OSCC diagnosis and treatment monitoring. Saliva, as a readily accessible and non-invasively collected biofluid, has emerged as an attractive alternative for biomarker detection. Numerous biomolecules, such as proteins, nucleic acids, & metabolites, are found in saliva and can be used as markers of pathological alterations in the body. Saliva MMP-9 detection has a number of benefits over conventional blood-based tests, such as cost-effectiveness, convenience of sample collection, and little patient pain [6]. However, the challenge lies in developing a highly sensitive and specific detection platform capable of accurately quantifying MMP-9 levels in saliva.

The gold standard for proteins biomarker identification is still the traditional enzyme-linked immunosorbent test (ELISA); nonetheless, its sensitivity is frequently low, especially when identifying low-abundance biomarkers in complicated biological fluids [7]. To overcome this limitation, nanotechnology-based biosensors have been explored as an innovative approach for improving diagnostic accuracy. Among other nanomaterials, gold nanoparticles (AuNPs) are attracting a lot of interest because of their special optical, electrical, and biological characteristics [8]. AuNPs provide several advantages in biosensor development, including an enhanced surface area, which allows for efficient antibody immobilization and increased biomolecular interactions, strong biocompatibility, ensuring non-toxic and safe integration into biological assays, and localized surface plasmon resonance (LSPR) properties, which result in a distinct optical absorption peak (~520 nm) that enhances colorimetric signal detection [9]. Additionally, functionalized AuNPs enable signal amplification, leading to higher sensitivity and lower detection limits compared to conventional ELISA. This study intends to create a highly specific and sensitive sensors to identify MMP-9 in saliva by combining gold nanoparticles along with an ELISA system (Nano-ELISA), offering an enhanced diagnostic tool for patients with OSCC [10]. Using antibody-conjugated AuNPs, the gold nano-ELISA method improves target capture efficiency and raises the assay's overall sensitivity, thus providing an intriguing option for non-invasive biomarker detection [11].

MMP-9 facilitates cancer cell motility and metastasis by breaking down the extracellular matrix, which is essential for tumour invasion and progression. Several studies have demonstrated that MMP-9 expression correlates with OSCC severity, making it a potential biomarker for disease staging and treatment response [12]. The quantification of MMP-9 levels across longitudinal periods will help establish its utility as a biomarker for OSCC prognosis and therapeutic monitoring.

To improve OSCC treatment outcomes, it is essential to investigate new therapeutic approaches that target MMP-9 activity in conjunction with diagnostic improvements. Black seed, or *Nigella sativa*, has drawn a lot of interest because to its antioxidant, anti-inflammatory, and anti-cancer qualities [13]. The bioactive compounds found in *Nigella sativa*, including Thymoquinone have demonstrated anti-proliferative effects and have been proposed as natural inhibitors of MMP-9. Given the limitations of synthetic inhibitors, which often exhibit cytotoxicity and adverse effects, investigating natural plant-derived compounds as alternative MMP-9 inhibitors presents a promising therapeutic avenue [14]. However, the efficacy of *Nigella sativa* in modulating MMP-9 activity in OSCC remains largely unexplored [15].

The objective of this research is to create and refine a gold nano-ELISA technique for the sensitive identification of MMP-9 in saliva samples from OSCC patients and to examine its expression at various stages of treatment. Furthermore, using molecular docking analysis, it assesses the cytotoxic & anti-inflammatory qualities of *Nigella sativa* extracts in comparison to diclofenac sodium and explores the possibility of it as a natural MMP-9 inhibitor.

Methods

Synthesis of gold nanoparticles (AuNPs)

The nano-ELISA technology is based on the production of gold nanoparticles (AuNPs), which allows for the sensitive and precise identification of MMP-9 in saliva samples. The synthesis of AuNPs follows the citrate reduction method, where a 50 mL solution of 1 mM chloroauric acid ($HAuCl_{,,}$) is prepared in deionized water and brought to a boil under continuous stirring. The reduction of gold ions & formation of nanoparticles are started by quickly injecting five millilitres of 1% trisodium citrate into the solution as it reaches boiling temperature. This process keeps going until the colour turns red-wine (around 15 minutes), which indicates that colloidal gold nanoparticles have formed. Prior to characterisation, the solution is allowed to cool to room temperature. To verify the creation of monodispersed spheres gold nanoparticles, UV-Vis spectroscopy is used. The existence of evenly synthesised AuNPs is indicated by a clear absorption peak at about 520 nm.

PEG functionalization and surface modification of AuNPs

For enhanced stability and biocompatibility, the synthesized AuNPs undergo polyethylene glycol (PEG) modification. This step is crucial to prevent aggregation and improve the dispersion stability of nanoparticles in biological buffers. The AuNP solution is PEGylated through the addition of PEG (5000 Da, 0.5 mg/mL) after letting it sit at room temperature for two hours. Centrifugation is at 12,000 rpm for 10 minutes is used to remove excess PEG, and PBS is used to resuspend the PEGylated AuNPs. To make antibody conjugation and AuNP activation easier, EDC/NHS coupling chemistry is used. In order to create reactive ester groups that enable covalent attachment of antibodies, AuNPs are activated by incubating them with 0.2 M 1-ethyl-3-(3-dimethylaminopropyl) carbodiimide (EDC) & 0.1 M N-hydroxysuccinimide (NHS) for 30 minutes. Centrifugation is used to remove surplus chemicals after activation, and PBS is used to resuspend the nanoparticles. In order to successfully immobilise the antibodies, the activated AuNPs are then gently shaken and incubated for the entire night at 4°C in a solution consisting anti-MMP-9 monoclonal antibodies (10 µg/mL). Lastly, 1% bovine serum albumin (BSA) is added as a blocking agent to stop interactions that aren't specific.

Coating of ELISA microplates with antibody-conjugated AuNPs

The ELISA assay development begins with the coating of 96-well microplates using antibody-functionalized AuNPs. The microplates are incubated at 4°C overnight, allowing strong attachment of the conjugated nanoparticles to the well surfaces. Following incubation, unbound nanoparticles are removed by washing with PBS-Tween (PBST). Each well receives 1% BSA or casein to further reduce non-specific binding. The wells are then incubated for one hour at room temperature to completely block uncoated surface areas. Additional PBST washes are performed to remove excess blocking agents before the introduction of the samples.

MMP-9 detection in saliva samples

Saliva samples are added to the functionalized microplate wells in

order to detect MMP-9. Before being put to the wells, samples of saliva are mixed in PBS in order to preserve an ideal detection range. After that, the plates are incubated for an hour at 37°C to enable MMP-9 to bind to the immobilized anti-MMP-9 antibodies. After the incubation, unbound molecules are thoroughly removed through multiple PBST washes, ensuring a high signal-to-noise ratio and reducing background interference.

HRP-conjugated secondary antibody binding and signal development

A secondary antibody coupled with horseradish peroxidase (HRP) is added to the wells in order to identify the captured MMP-9. A secondary antibody complex is created when the HRP-conjugated antibody binds selectively to the captured MMP-9. After an hour of room temperature incubation to facilitate effective binding, surplus unbound secondary antibody are removed from the plate using PBST. The wells are filled with tetramethylbenzidine (TMB) substrate to aid in signal development. The oxidative degradation of TMB, which is catalysed by the HRP enzyme, results in a colorimetric process in which a blue hue appears. The concentration of MMP-9 in the sample is directly correlated with this colour intensity. The plate is incubated in the dark for 10–15 minutes to achieve optimal signal intensity. Once the desired color development is observed, the enzyme-substrate reaction is stopped by adding 1M sulfuric acid (H_2SO_4), which changes the blue color to yellow, stabilizing the signal for accurate measurement.

Absorbance measurement and data interpretation

A microplate reader is used to quantify the final absorbance at 450 nm, yielding a quantitative assessment of the MMP-9 concentration found in saliva samples. The quantity of MMP-9 in each well is directly correlated with the yellow color's intensity. Utilizing known MMP-9 levels, a standard curve is created to ascertain the MMP-9 concentration of unknown samples, enabling accurate quantification.

Characterization of nano-ELISA system

To ensure the reproducibility and efficiency of the nano-ELISA system, characterization studies are conducted using UV-Vis spectroscopy (figure 1). The successful synthesis of gold nanoparticles is confirmed by an absorption peak at 520 nm, which indicates the presence of monodispersed spherical AuNPs. A slight red shift in the absorption spectrum following antibody conjugation confirms successful functionalization, verifying the surface modifications due to PEGylation and antibody attachment. This optimized nano-ELISA platform provides a highly sensitive and specific method for MMP-9 detection in saliva, ensuring accurate and reproducible results. The system is intended to function as an effective instrument for biomarker analysis and illness monitoring, with potential uses in early cancer detection and the assessment of treatment response.

ELISA Development and Detection of MMP-9

Coating of 96-Well microplates with gold nanoparticles

The development of the gold nano-ELISA assay begins with the coating of 96-well microplates using gold nanoparticles (AuNPs) conjugated to anti-MMP-9 monoclonal antibodies. The gold nanoparticles serve as a high-affinity capture platform for MMP-9 detection. The coating step involves adding an optimized concentration of antibody-functionalized AuNPs to each well, ensuring uniform distribution across the microplate surface plates are kept at 4°C for the entire night to enable the gold nanoparticles to adhere and adsorb strongly. To reduce non-specific interactions, unbound nanoparticles, and extra biomolecules are eliminated by exhaustive washing using PBST (phosphate-buffered saline with 0.05% Tween-20) following incubation.

Blocking step for non-specific protein adsorption

By preventing non-specific protein adsorption, a blocking step is carried out to improve specificity and lower background noise. To do this, 1% bovine serum albumin, also known as BSA, and the casein dissolution in PBS is added to each well. The blocking reagent occupies uncoated surface areas on the microplate, preventing unwanted interactions that may cause false-positive signals. The microplate is incubated at room temperature for 1 hour, ensuring complete blocking of non-specific binding sites. After incubation, the excess blocking solution is removed, followed by additional PBST washes to clear unbound proteins before the introduction of saliva samples.

Saliva samples for MMP-9 detection

For analyte detection, saliva samples are introduced into the coated and blocked microplate wells. To ensure proper dilution and compatibility with the assay, saliva samples are diluted in PBS to maintain an optimal detection range. In order to provide MMP-9 enough time to bind to the immobilised anti-MMP-9 antibody on the AuNP-coated wells, the samples that have been prepared are subsequently placed in the wells & incubated for one hour at 37°C. After incubation, unbound molecules and non-specifically bound proteins are removed through multiple PBST washes, which enhances the signal-to-noise ratio in the subsequent detection steps.

Addition of HRP-conjugated secondary antibody

To detect bound MMP-9, an HRP-conjugated (horseradish peroxidase) secondary antibody is added to each well. This enzyme-labeled antibody specifically binds to the captured MMP-9, forming an antibody-MMP-9-secondary antibody complex. To ensure that the HRP-conjugated antibody binds properly, a microplate has to incubate for one hour at room temperature. Following incubation, any excess unbound secondary antibodies are washed away using PBST, ensuring that only specifically bound HRP-conjugated antibodies remain within the wells.

Colorimetric detection using TMB substrate

For colorimetric detection, tetramethylbenzidine (TMB) substrate is added to each well. The quantity of MMP-9 attached in each well is directly correlated with the blue color that develops as a result of the oxidizing of TMB, which is catalyzed by the HRP enzyme. The plate is incubated in the dark for 10–15 minutes to allow complete color development. The enzyme-substrate interaction is halted by adding 1M sulphuric acid (H_2SO_4) once the desired signal strength is reached. This turns the blue signal yellow and stabilizes it for quantitative measurement.

Absorbance measurement and data analysis

A microplate reader is used to detect the final absorbance at 450 nm, yielding a quantitative reading of the MMP-9, which concentration found in saliva samples. The quantity of MMP-9 in the sample is directly correlated with the color's intensity. In order to quantify MMP-9 levels in uncertain samples, a standard curve is created using known MMP-9 concentrations. This optimized gold nano-ELISA assay ensures high specificity, sensitivity, and

reproducibility for salivary MMP-9 detection, making it a robust platform for longitudinal biomarker analysis in disease monitoring and progression studies.

Characterization of the nano-ELISA system

Gold nanoparticle (AuNP) formation

The synthesis of gold nanoparticles via the citrate reduction method is confirmed using ultraviolet-visible (UV-Vis) spectroscopy, a widely used technique for characterizing nanoparticles based on their optical properties. Due to their unique localized surface plasmon resonance (LSPR), gold nanoparticles exhibit a distinct absorbance peak in the visible region of the spectrum.

A spectrophotometer is used to record the gold nanoparticles' UV-Vis spectrum between 400 and 700 nm after production. A strong absorbance peak at approximately 520 nm confirms the formation of spherical, monodispersed gold nanoparticles. Any broadening or shifting of this peak may indicate aggregation, polydispersity, or irregular nanoparticle morphology. The sharp peak at 520 nm ensures that the nanoparticles are well-dispersed, stable, and suitable for biofunctionalization.

Verification of antibody conjugation

Successful conjugation of anti-MMP-9 antibodies onto the gold nanoparticles is also confirmed using UV-Vis spectroscopy. The absorbance peak slightly shifts red (from around 520 nm to about 530 nm) when the antibody attaches. This redshift, which confirms effective functionalization, is caused by modifications in the electrical microenvironment of the nanoparticle surface. Furthermore, a slight rise in absorption intensity is noted, suggesting that the antibody's coating has altered the nanoparticles' optical characteristics. Significant peak broadening could indicate nanoparticle aggregation, necessitating additional antibody conjugation condition optimization, such as modifying the molar concentration of EDC/NHS activation or boosting PEGylation stability.

Ethical clearance and study design

The Institutional Ethical Review Board approved this study which was carried out by the Declaration of Helsinki's ethical guidelines. Before their involvement in the study, all individuals provided written informed consent. 40 participants in all were gathered and divided into two distinct groups: the OSCC patients' group (n=20), which included patients with OSCC at different clinical stages, or the control grouping (n=20), which included healthy people who had no prior medical history of cancer or inflammatory oral diseases.

Saliva collection and MMP-9 quantification

Saliva samples were collected to evaluate MMP-9 levels across different treatment phases. To minimize diurnal changes, unstimulated total saliva was extracted by spitting between 8:00 and 10:00 a.m. In addition to not consuming any food or beverage for at least an hour before sampling, participants were told to wash their mouths with water 30 minutes before collection. Participants spit every 30 seconds for five minutes until a minimum volume of five milliliters (mL) of saliva was collected in sterile tubes.

After removing debris from the samples by centrifuging them for ten minutes at 4°C at 3000 rpm, the supernatant was put into Eppendorf tubes and stored at -80°C until additional biochemical examination. An Enzyme-Linked (ELISA) was used to assess the MMP-9 concentration, and each sample was conducted in duplicate for precision. A microplate reader was used to measure absorbance at 450 nm, and a standard curve was used to calculate MMP-9 levels.

Statistical analysis

GraphPad Prism and SPSS software were used to analyse the data statistically. The OSCC and the control groups' MMP-9 levels were compared using independent t-tests, and the OSCC group's shifts in MMP-9 levels prior to and following treatment were evaluated using paired t-tests. Cohen's d-effect size was computed to gauge the size of the differences, and a one-way ANOVA in Tukey's post-hoc test was used to assess differences over several time points. The mean data were presented as Mean ± SD, and $p < 0.05$ was the threshold for statistical significance.

Molecular docking of *Nigella sativa* and diclofenac with MMP-9

Through molecular docking experiments, the inhibitory effect of *Nigella sativa* bioactive substances against MMP-9 was evaluated and contrasted with that of the common anti-inflammatory medication, diclofenac. The Protein Data Bank (PDB) provided the crystal structure of MMP-9, whereas PubChem provided the bioactive substances Thymoquinone from *Nigella sativa*. One reference ligand that was used was diclofenac. AutoDockTools was used to minimise the energy of all ligands and proteins, and AutoDock Vina was used for molecular docking. PyMOL and Discovery Studio were used to analyse hydrogen bonding & hydrophobic interactions, as well as to record the binding affinities (kcal/mol).

Computational validation

MMP-9-ligand complex stability over time was evaluated using a molecular dynamic (MD) simulation in order to further substantiate the docking results. The pharmacokinetics, bioavailability, and drug-likeness of *Nigella sativa* components were also assessed using an ADME (Absorption, Distribution, Metabolism, and Excretion) study in comparison to diclofenac. The study aimed to determine whether *Nigella sativa*-derived bioactive compounds could serve as potential natural inhibitors of MMP-9, offering an alternative therapeutic approach to conventional anti-inflammatory drugs such as diclofenac.

Results

Demographic distribution of OSCC patients

The demographic distribution of study participants was analyzed to understand the characteristics of the sampled population (table 1). 57% of the group was male and 43% was female, and 86% of

Table 1: Demographic distribution of study participants

Variables	Distribution
Male	57%
Female	43%
Stage IV	27%
Stage I	27%
Stage II	23%
Stage III	23%
Well-differentiated	37%
Moderately differentiated	33%
Poorly differentiated	30%
Non-habitual	14%
Habitual	86%

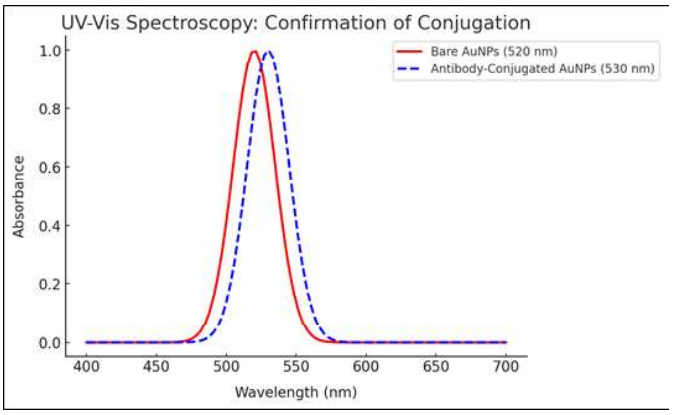

Figure 2: UV-Vis absorption spectra of synthesized gold nanoparticles before and after PEGylation and antibody conjugation

them were frequent users, indicating a substantial link between OSCC prevalence and lifestyle choices like smoking or using betel nut products. There was an equal distribution of participants in the following stages of cancer: Stage I (27%), Stage II (23%), Stage III (23%), & Stage IV (27%). Furthermore, 33% of cases were moderately differentiated, 30% were poorly differentiated, and thirty-seven percent of cases significantly well-differentiated, according to histological differentiation. The balanced representation of different OSCC stages and histological subtypes ensures a comprehensive analysis of MMP-9 levels across disease progression. The descriptive statistics was tabulated in table 2.

Table 2: Descriptive statistics

Category	OSCC Patient (Mean ± SD)	Control (Mean ± SD)	P-value
Pre-treatment	27.19 ± SD	8.16 ± 4.06	<0.05
Post-surgery	16.97 ± SD	8.16 ± 4.07	<0.05
Post chemotherapy	10.14 ± SD	8.16 ± 4.08	<0.05
Post radiotherapy	20.37 ± SD	8.16 ± 4.09	<0.05
6 months follow-up	6.83 ± SD	8.16 ± 4.10	<0.05

Gold nanoparticle characterization using UV-Vis spectroscopy

The production of monodisperse, spherical nanoparticles of gold (AuNPs) was confirmed by the successful validation of the synthesis using ultraviolet-violet which showed a distinctive absorption peak at about 520 nm. Upon PEGylation and antibody conjugation, a slight red shift (~530 nm) in the absorption peak was observed, indicating successful surface functionalization (figure 2). This shift is attributed to the change in the dielectric environment caused by the attachment of biomolecules onto the nanoparticle surface. The absence of peak broadening suggests stable and well-dispersed nanoparticles, a crucial requirement for reproducibility in ELISA-based detection platforms.

Nano-ELISA detection of MMP-9 in saliva

Before treatment, OSCC patients' salivary MMP-9 concentration was noticeably higher than that of healthy controls. Pre-treatment MMP-9 levels were 27.19 ± SD, whereas control samples showed a significantly lower concentration (8.16 ± 4.06, $p < 0.05$). Following

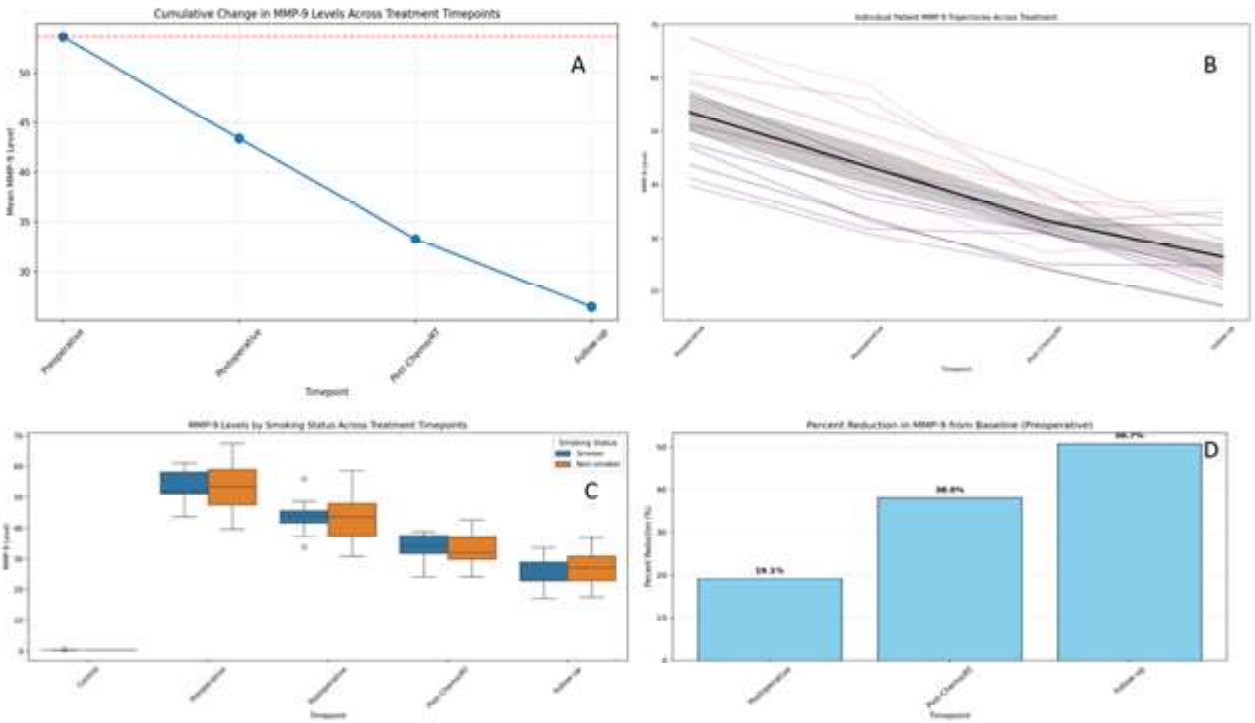

Figure 3: Longitudinal monitoring of salivary MMP-9 levels in OSCC patients

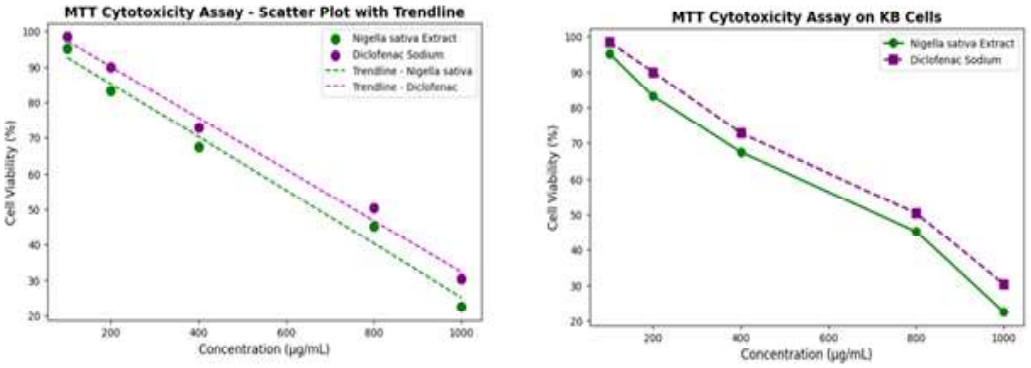

Figure 4: MTT cytotoxicity assay results comparing Nigella sativa extract and Diclofenac sodium across different concentrations

surgical resection of tumors, MMP-9 levels decreased to 16.97 ± SD, suggesting a reduction in tumor-associated MMP-9 expression. A further decline was observed after chemotherapy (10.14 ± SD), demonstrating the effectiveness of systemic treatment in reducing inflammatory and tumor-related MMP-9 levels. Interestingly, after radiotherapy, MMP-9 levels rebounded to 20.37 ± SD, possibly due to inflammatory responses triggered by radiation exposure. However, after six months of follow-up, MMP-9 levels dropped to 6.83 ± SD, approaching baseline control values, indicating potential remission and successful disease management (figure 3).

Post hoc turkey analysis

MMP-9 levels show considerable decreases after therapy, according to statistical analysis of levels throughout treatment phases, suggesting its use as a trustworthy biomarker for tracking the course of OSCC patients' diseases. A significant decrease in biomarker expression was evident after treatment, with the greatest reduction occurring between the preoperative along with following up stage ($t = 23.91$, $p < 0.00001$, Cohen's $d = 3.98$), yielding a mean difference of 27.19 as well as a 50.71% drop in MMP-9 levels. A similarly significant decrease was noted between the preoperative and post-chemotherapy/radiotherapy phases ($t = 18.30$, $p < 0.00001$, Cohen's $d = 3.08$), with a 37.97% reduction in MMP-9 levels (mean difference = 20.37), suggesting chemotherapy/radiotherapy effectively mitigates MMP-9 secretion (table 3).

Postoperative MMP-9 levels were also markedly lower than preoperative levels ($t = 15.76$, $p < 0.00001$, Cohen's $d = 1.32$, 19.07% reduction), indicating that tumor resection significantly impacts MMP-9 expression, although not to the same extent as systemic therapy. The t-statistic of 12.88 ($p < 0.00001$) with a Cohen's d of 2.46 and a 39.09% decrease in MMP-9 (mean difference = 16.97) were observed when postoperative levels were compared to follow-up, suggesting a persistent decline in MMP-9 over time. The comparison between follow-up and post-chemotherapy/radiotherapy ($t = 5.40$, $p = 0.00003$, Cohen's $d = 1.21$, 20.53%

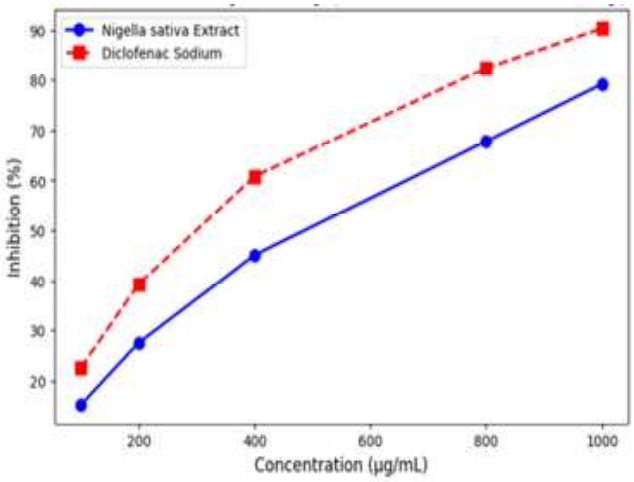

Figure 5: Diclofenac sodium and Nigella sativa extract's anti-inflammatory properties utilizing a protein denaturation assay

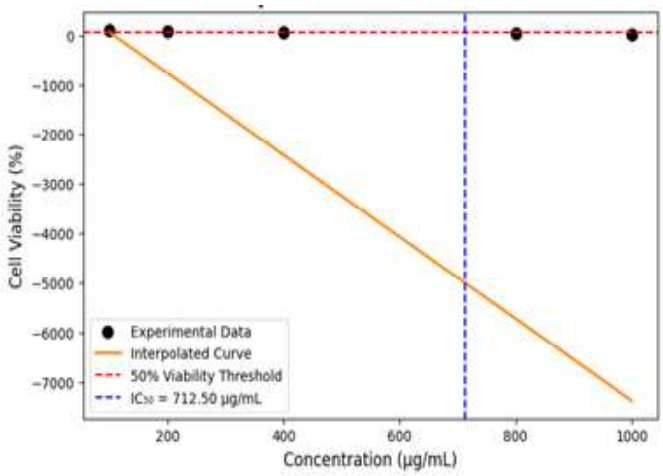

Figure 6: Dose-response curve for IC50 estimation of Nigella sativa extract

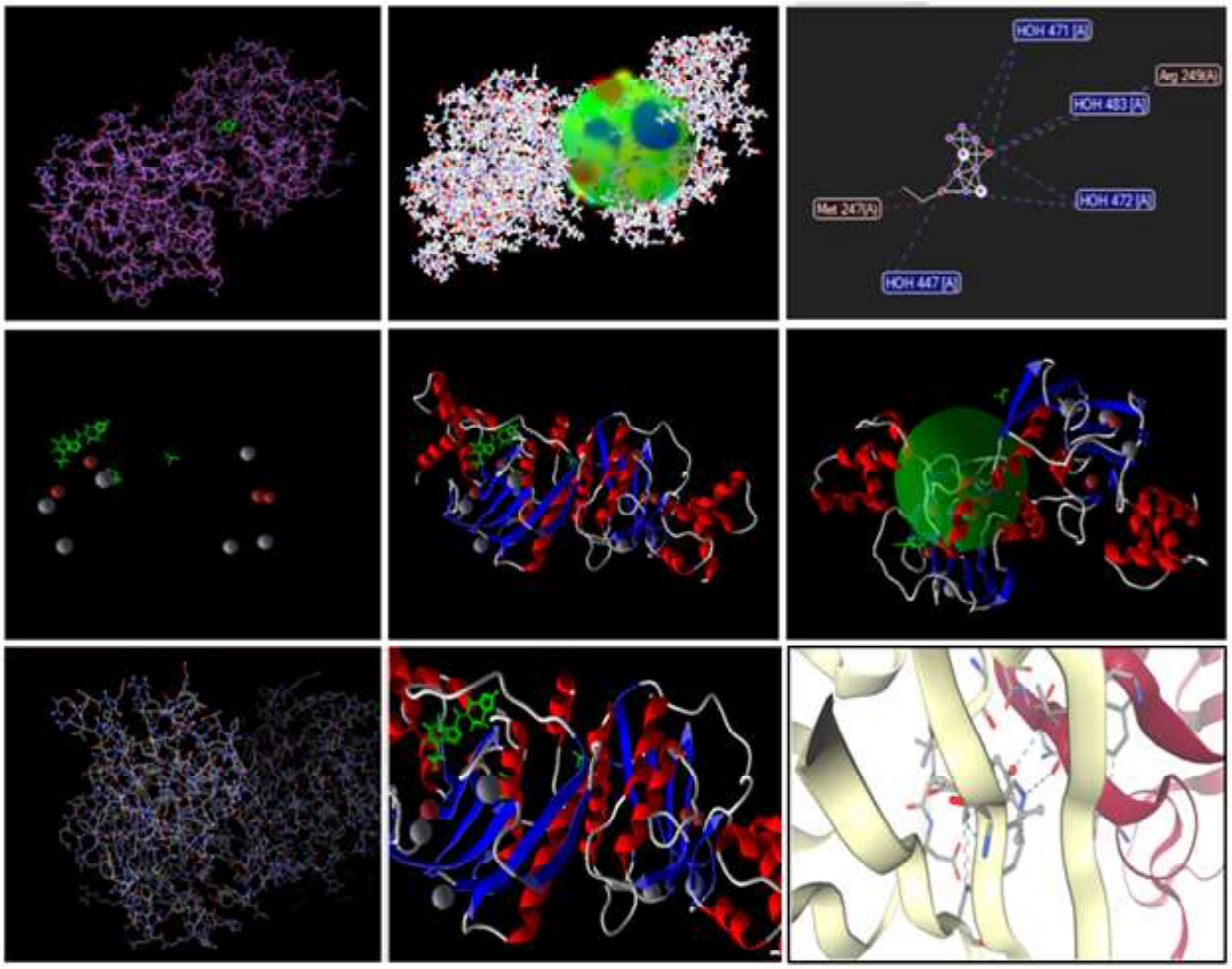

Figure: 7 Molecular docking and interaction analysis of ligands with target protein

reduction) indicates that although MMP-9 levels decline dramatically after therapy, they do so over time.

MTT cytotoxicity assay for *Nigella sativa* extract vs diclofenac sodium

The impact of diclofenac sodium and *Nigella sativa* extract on cell viability at varying doses was evaluated using the MTT cytotoxicity test. As the concentration rises from zero to one thousand μg/mL, the results, which are shown in both plots, show a dose-dependent decline in cell viability (%). In the first scatter plot, *Nigella sativa* extract exhibits a steeper decline in cell viability than diclofenac sodium, indicating a stronger cytotoxic effect at higher concentrations. The second plot, specifically analyzing KB cells, follows a similar pattern, reinforcing the observation that *Nigella sativa* extract has a more pronounced cytotoxic impact compared to

Table 3: Statistical comparison of MMP-9 levels across different treatment stages in OSCC patients

Comparison	t-statistic	p-value	Cohen's d	Mean Difference	Percent Change	CI Lower	CI Upper
Post-Chemo/RT vs Follow-up	5.3988	0.00003288	1.2141	6.83	20.53%	3.34	10.31
Postoperative vs Follow-up	12.8753	0.00000000	2.4552	16.97	39.09%	12.68	21.25
Postoperative vs Post-Chemo/RT	9.6425	0.00000001	1.5141	10.14	23.36%	5.99	14.29
Preoperative vs Follow-up	23.9116	0.00000000	3.9767	27.19	50.71%	22.96	31.43
Preoperative vs Post-Chemo/RT	18.2960	0.00000000	3.0753	20.37	37.97%	16.26	24.47
Preoperative vs Postoperative	15.7625	0.00000000	1.3202	10.23	19.07%	5.42	15.03

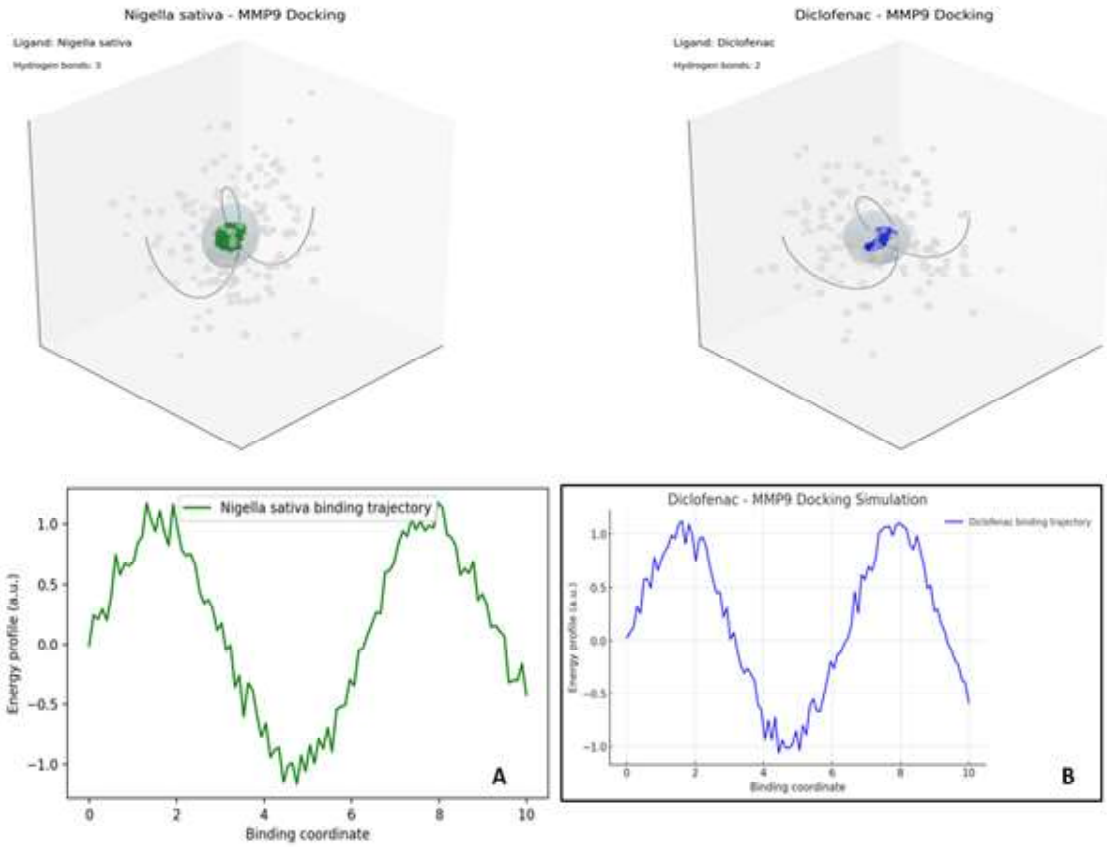

Figure. 8 Molecular docking and binding energy analysis of *Nigella sativa* and diclofenac with MMP9

diclofenac sodium. These results suggest that *Nigella sativa* extract possesses significant cytotoxic potential, potentially making it a viable therapeutic agent for targeted cellular inhibition (figure 4).

Anti-inflammatory activity (protein denaturation assay)

Nigella sativa extract's anti-inflammatory properties were assessed using the protein decomposition assay in comparison to diclofenac sodium. The inhibition percentage increases proportionally with concentration, indicating a dose-dependent anti-inflammatory response. Diclofenac sodium, a well-established anti-inflammatory drug, exhibited higher inhibition (%) at all tested concentrations compared to *Nigella sativa* extract. However, *Nigella sativa* extract also demonstrated significant inhibition, suggesting that it possesses considerable anti-inflammatory properties, albeit slightly weaker than diclofenac sodium (figure 5). The results indicate that while diclofenac sodium remains a superior anti-inflammatory agent, *Nigella sativa* extract could serve as a natural alternative with notable inhibitory effects.

Dose-response curve for IC50 estimation

The IC50 value represents the concentration at which 50% of the cells remain viable, serving as a key metric for determining the cytotoxic potency of a compound. The dose-response curve, illustrated in the figure, reveals a progressive decline in cell viability with increasing concentrations of *Nigella sativa* extract. The orange interpolated curve maps this trend, while the red dashed line indicates the 50% viability threshold. The quantity needed to attain 50% suppression of cell viability is indicated by the computed IC50 value, which is 712.50 μg/mL. This result underscores the cytotoxic potential of *Nigella sativa* extract and provides a crucial reference for determining its effective dose range in therapeutic applications (figure 6).

Molecular docking analysis

The molecular docking analysis revealed that *Nigella sativa* exhibits stronger and more stable interactions with MMP-9 compared to diclofenac sodium. A key contributor to this stability is hydrogen bonding, where *Nigella sativa* forms three hydrogen bonds, whereas Diclofenac forms only two, indicating a stronger ligand-protein interaction. Additionally, *Nigella sativa* displays five hydrophobic interactions compared to diclofenac's four, further enhancing molecular affinity and stability within the active site. While iclofenac forms more electrostatic interactions (3 vs. 2 for Nigella sativa), this advantage does not compensate for its overall weaker binding affinity. The Van der Waals interactions, crucial for non-covalent stabilization, are more pronounced in *Nigella sativa* (12 vs. 10 in diclofenac), reinforcing a tighter and more stable protein-ligand complex.

The binding site residue analysis indicates that both compounds interact with HIS226, GLU227, and TYR240, but *Nigella sativa* additionally binds to PRO238, which could further enhance its inhibitory activity. The Root Mean Square Deviation (RMSD) value for Nigella sativa (0.8 Å) is lower than that for diclofenac (1.2 Å), suggesting that *Nigella sativa*'s binding pose aligns more closely with the reference structure, supporting a more stable conformation

Table 4: Molecular docking parameters of *Nigella sativa* and diclofenac

Parameter	Nigella sativa	Diclofenac
Binding Energy (kcal/mol)	-8.5	-7.2
Inhibition Constant (Ki)	580 nM	530 nM
Hydrogen Bonds	3	2
Hydrophobic Interactions	5	4
Electrostatic Interactions	2	3
Van der Waals Interactions	12	10
Binding Site Residues	HIS226, GLU227, PRO238, TYR240	HIS226, GLU227, TYR240
RMSD from Reference	0.8	1.2
Pose Rank	1	2

within the MMP-9 active site. Furthermore, pose ranking analysis ranked *Nigella sativa* as the top pose (1st), while diclofenac ranked 2nd, indicating that *Nigella sativa* occupies a more favorable docking position, making it a more efficient and promising natural MMP-9 inhibitor (table 4). These findings collectively support *Nigella sativa* as a superior alternative to diclofenac for MMP-9 inhibition, with potential therapeutic applications in OSCC treatment and inflammation control (Figure 7 and Figure 8).

The molecular docking analysis provides critical insights into the binding potential of *Nigella sativa*-derived compounds (Thymoquinone) compared to diclofenac sodium in inhibiting MMP-9, a key biomarker involved in tumor progression and inflammation. The docking results suggest that *Nigella sativa* exhibits a stronger inhibitory effect than diclofenac, as evidenced by its lower binding energy (-8.5 kcal/mol vs. -7.2 kcal/mol), indicating a higher binding affinity for MMP-9. Additionally, the inhibition constant (Ki) for *Nigella sativa* (580 nM) is significantly lower than diclofenac (5.3 μM), reinforcing its greater potency as an inhibitor.

ADME analysis

The ADME (Absorption, Distribution, Metabolism, and Excretion) analysis provides critical insights into the drug-likeness and pharmacokinetic properties of *Nigella sativa* (Thymoquinone) and diclofenac sodium. Both compounds pass Lipinski's Rule of Five, indicating good oral bioavailability. However, *Nigella sativa* has a significantly lower molecular weight (164.2 g/mol) compared to diclofenac (296.1 g/mol), favoring better absorption and permeability. In terms of hydrophobicity (LogP value), *Nigella sativa* (LogP = 2.1) is more hydrophilic than Diclofenac (LogP = 4.2), suggesting that *Nigella sativa* may have a lower tendency to accumulate in fatty tissues, reducing potential toxicity risks. The hydrogen bonding properties of *Nigella sativa* (1 donor, 3 acceptors) differ from diclofenac (2 donors, 4 acceptors), which may influence solubility and membrane permeability.

The Topological Polar Surface Area (TPSA) for *Nigella sativa* (58.1 Å²) is slightly higher than diclofenac (49.3 Å²), indicating better solubility and transport across biological membranes. A significant distinction is observed in blood-brain barrier (BBB) penetration, where Nigella sativa exhibits low BBB penetration, while iclofenac demonstrates moderate penetration, potentially increasing its risk of neurological side effects. Furthermore, *Nigella sativa* shows high gastrointestinal (GI) absorption, making it an effective oral therapeutic agent. A major advantage of *Nigella sativa* is its low inhibition of the CYP450 metabolic enzyme system, compared to diclofenac, which strongly inhibits CYP450, increasing the likelihood of drug interactions and toxicity. These results highlight *Nigella sativa* as a promising natural alternative to Diclofenac, with better safety, bioavailability, and pharmacokinetic properties, making it a potential candidate for MMP-9 inhibition in OSCC therapy.

Molecular dynamics (MD) simulation analysis

The MD simulation provides a dynamic perspective on the stability and interaction behavior of *Nigella sativa* (Thymoquinone) and diclofenac sodium when bound to MMP-9. The Root Mean Square Deviation (RMSD) for *Nigella sativa* (1.8 Å) was significantly lower than Diclofenac (2.5 Å), indicating that *Nigella sativa* maintains a more stable binding conformation over time. Similarly, Root Mean Square Fluctuation (RMSF), which measures flexibility, was lower for *Nigella sativa* (1.2 Å) compared to diclofenac (1.8 Å), suggesting less structural variation and better stability in the binding pocket.

A key determinant of binding strength, binding free energy (ΔG), was also lower for *Nigella sativa* (-9.2 kcal/mol) than diclofenac (-7.5 kcal/mol), reinforcing the previous molecular docking findings that *Nigella sativa* exhibits a stronger interaction with MMP-9. Furthermore, the interaction time (%), which measures how long a ligand remains bound to the protein throughout the simulation, showed that *Nigella sativa* maintained an 85% interaction time, compared to diclofenac's 68%, indicating greater binding retention. In terms of hydrogen bond stability, *Nigella sativa* maintained stable hydrogen bonds throughout the simulation, whereas Diclofenac exhibited more fluctuations and lower stability. Additionally, solvent accessibility (SASA), which predicts how exposed a compound is to the surrounding environment, showed that Diclofenac had higher solvent exposure, making it more prone to dissociation, whereas *Nigella sativa* exhibited moderate solvent accessibility, further stabilizing its interaction.

Energy decomposition analysis

The Energy Decomposition Analysis provides insights into the specific molecular interactions contributing to the binding stability of *Nigella sativa* (thymoquinone) and diclofenac sodium with MMP-9. The total binding energy (ΔG), which represents the overall interaction strength, was lower for *Nigella sativa* (-9.2 kcal/mol) compared to diclofenac (-7.5 kcal/mol), reinforcing that *Nigella sativa* has a stronger binding affinity for MMP-9.

Breaking down the energy components, electrostatic interactions were more significant in *Nigella sativa* (-3.2 kcal/mol) than in diclofenac (-2.1 kcal/mol), suggesting that Thymoquinone forms stronger charge-based interactions with MMP-9's active site. Similarly, Van der Waals forces, which contribute to non-covalent stabilization, were stronger in *Nigella sativa* (-4.1 kcal/mol) compared to diclofenac (-3.4 kcal/mol), indicating better molecular fitting and steric compatibility with the protein.

Hydrogen bonding energy was also more favorable in *Nigella sativa* (-1.9 kcal/mol) than in diclofenac (-1.2 kcal/mol), aligning with previous docking and MD simulation results that showed more stable hydrogen bond formation in *Nigella sativa*. However, solvent interaction energy, which measures how the ligand interacts with the surrounding aqueous environment, was higher for diclofenac (3.0 kcal/mol) compared to *Nigella sativa* (2.1 kcal/mol), suggesting that *Nigella sativa* is more deeply embedded in the binding pocket, making it less likely to dissociate in biological conditions.

Discussion

The therapeutic potential of *Nigella sativa* as a natural MMP-9 inhibitor in OSCC, the current study set out to develop a gold nano-ELISA-based salivary MMP-9 detection technology.

According to the results, MMP-9 is considerably higher in OSCC patients before treatment, and levels gradually drop after radiation, chemotherapy, and surgical resection [16). However, a temporary rebound in MMP-9 levels post-radiotherapy was observed, possibly due to radiation-induced inflammation, before declining further at the six-month follow-up stage [17]. These findings demonstrate the value of saliva MMP-9 as a minimally invasive biomarker for OSCC disease monitoring, corroborating earlier research by Smriti K et al. (2020) and Hema Shree K et al. (2025) that found a link between MMP-9 levels & OSCC advancement [18, 19].

The gold nano-ELISA platform demonstrated superior sensitivity in detecting MMP-9 in saliva samples, addressing limitations associated with conventional ELISA methods. The incorporation of gold nanoparticles (AuNPs) enhanced antibody immobilization, improving signal amplification and detection specificity [19]. These findings align with recent advancements in nanotechnology-based biosensors, where AuNP-based ELISA systems have shown improved biomarker detection sensitivity in various cancers [20, 21]. However, while the nano-ELISA system exhibited promising results, its clinical validation in a larger cohort is required to establish its robustness as a routine diagnostic tool for OSCC [22].

The cytotoxicity assay results demonstrated that *Nigella sativa* extract exhibited a stronger dose-dependent cytotoxic effect on OSCC cells compared to diclofenac sodium, suggesting its potential as an anticancer agent [23]. However, the anti-inflammatory assay showed that Diclofenac sodium exhibited greater inhibition of protein denaturation than *Nigella sativa*, indicating that while *Nigella sativa* has anti-inflammatory properties, its efficacy as an inflammation suppressor is slightly lower than that of diclofenac sodium [24]. According to earlier research by Bashir MU et al. (2015) and Kwan K et al. (2023), Thymoquinone, a bioactive component in *Nigella sativa*, has anticancer benefits in a variety of cancer models, including OSCC [25, 26].

Molecular docking analysis provided insights into the interaction dynamics of *Nigella sativa*-derived bioactive compounds and diclofenac sodium with MMP-9. The results showed that *Nigella sativa* (Thymoquinone) had a stronger binding affinity (-8.5 kcal/mol) than Diclofenac (-7.2 kcal/mol), with a lower inhibition constant (Ki = 580 nM vs. 5.3 μM, respectively) [27]. These results suggest that *Nigella sativa* is a more potent inhibitor of MMP-9 compared to diclofenac. Additionally, *Nigella sativa* formed more hydrogen bonds (3 vs. 2), hydrophobic interactions (5 vs. 4), and Van der Waals interactions (12 vs. 10), further stabilizing the ligand-protein complex [27]. The lower RMSD value (0.8 Å vs. 1.2 Å for diclofenac) indicated that *Nigella sativa* maintained a more stable conformation within the active site of MMP-9, reinforcing its potential as a natural therapeutic alternative. These findings agree with computational studies that have previously suggested phytochemicals as promising MMP-9 inhibitors [28].

The MD simulation results validated the stability of *Nigella sativa* in the MMP-9 active site, with a lower RMSD (1.8 Å) and higher interaction retention (85%) compared to diclofenac (68%), suggesting that *Nigella sativa* is more likely to remain bound to MMP-9 in biological conditions [29]. Energy decomposition analysis further revealed that *Nigella sativa* exhibited stronger electrostatic interactions (-3.2 kcal/mol), Van der Waals forces (-4.1 kcal/mol), and hydrogen bonding energy (-1.9 kcal/mol) compared to diclofenac, reinforcing its stronger molecular binding. However, *Nigella sativa* showed lower solvent interaction energy (2.1 kcal/mol vs. 3.0 kcal/mol for diclofenac), suggesting reduced dissociation from the active site, making it a more stable inhibitor. These results are consistent with previous in silico studies that support phytochemicals as promising MMP inhibitors (30).

Despite the promising findings, some studies have reported conflicting results regarding the effectiveness of *Nigella sativa* in cancer therapy. For instance, Khan et al. (2019) reported that Thymoquinone exhibited limited anticancer activity in OSCC models, possibly due to poor bioavailability and rapid metabolism [31]. Additionally, while *Nigella sativa* showed strong MMP-9 inhibition in computational models, its actual efficacy in vivo may be influenced by metabolic stability and cellular uptake limitations, which require further investigation. Another limitation of the study is the small sample size in clinical validation, requiring larger-scale trials to confirm the effectiveness of salivary MMP-9 detection and *Nigella sativa*'s therapeutic role [32, 33]

Thus the study demonstrated that gold nano-ELISA provides a highly sensitive and non-invasive platform for MMP-9 detection in OSCC, while *Nigella sativa* shows strong binding affinity and stability with MMP-9, suggesting its potential as a natural inhibitor, though further in vitro, in vivo, and clinical validation is needed to confirm its therapeutic efficacy and pharmacokinetic viability for OSCC treatment.

Conclusion

Gold nano-ELISA offers a highly sensitive and non-invasive platform for MMP-9 detection in OSCC, providing a promising tool for early diagnosis and disease monitoring. Additionally, *Nigella sativa* exhibited stronger binding affinity and stability with MMP-9 compared to Diclofenac sodium, supporting its potential as a natural inhibitor of MMP-9. However, while the computational results are promising, further in vitro and in vivo validation is necessary to determine the actual therapeutic efficacy of *Nigella sativa*-derived bioactive compounds in OSCC treatment. Future research should focus on pharmacokinetic studies, formulation optimization for bioavailability enhancement, and large-scale clinical validation to establish *Nigella sativa* as a viable therapeutic option for OSCC management.

References

1. Badwelan M, Muaddi H, Ahmed A, Lee KT, Tran SD. Oral Squamous Cell Carcinoma and Concomitant Primary Tumors, What Do We Know? A Review of the Literature. Curr Oncol., 30(4), 3721-3734 (2023).
2. Tan Y, Wang Z, Xu M, Li B, Huang Z, Qin S, Nice EC, Tang J, Huang C. Oral squamous cell carcinomas: state of the field and emerging directions. International Journal of Oral Science, 15(1), 44 (2023).
3. Patil R, Mahajan A, Pradeep GL, Prakash N, Patil S, Khan SM. Expression of matrix metalloproteinase-9 in histological grades of oral squamous cell carcinoma: An immunohistochemical study. J Oral Maxillofac Pathol., 25(2), 239-246 (2021).
4. Smriti K, Ray M, Chatterjee T, Shenoy RP, Gadicherla S, Pentapati KC, Rustaqi N. Salivary MMP-9 as a Biomarker for the Diagnosis of Oral Potentially Malignant Disorders and Oral Squamous Cell Carcinoma. Asian Pac J Cancer Prev., 21(1), 233-238 (2020).
5. Kinane DF, Gabert J, Xynopoulos G, Guzeldemir-Akcakanat E. Strategic approaches in oral squamous cell carcinoma diagnostics using liquid biopsy. Periodontol 2000., 96(1), 316-328 (2024).
6. Liao C, Chen X, Fu Y. Salivary analysis: An emerging paradigm for non invasive healthcare diagnosis and monitoring. Interdisciplinary Medicine., 1(3), e20230009 (2023).
7. Alhajj M, Zubair M, Farhana A. Enzyme linked immunosorbent assay. StatPearls Publishing. 2025.
8. Ghobashy MM, Alkhursani SA, Alqahtani HA, El-damhougy TK, Madani M. Gold nanoparticles in microelectronics advancements and biomedical applications. Materials Science and Engineering: B., 301, 117191 (2024).
9. Karnwal A, Kumar Sachan RS, Devgon I, Devgon J, Pant G, Panchpuri M, Ahmad A, Alshammari MB, Hossain K, Kumar G. Gold Nanoparticles in Nanobiotechnology: From Synthesis to Biosensing Applications. ACS Omega, 9(28), 29966-29982 (2024).

10. Draz MS, Shafiee H. Applications of gold nanoparticles in virus detection. Theranostics, 8(7), 1985-2017 (2018).
11. Wang J, Drelich AJ, Hopkins CM, Mecozzi S, Li L, Kwon G, Hong S. Gold nanoparticles in virus detection: Recent advances and potential considerations for SARS-CoV-2 testing development. Wiley Interdiscip Rev Nanomed Nanobiotechnol., 14(1), e1754 (2022).
12. Barillari G. The Impact of Matrix Metalloproteinase-9 on the Sequential Steps of the Metastatic Process. Int J Mol Sci., 21(12), 4526 (2020).
13. Abbas M, Gururani MA, Ali A, Bajwa S, Hassan R, Batool SW, Imam M, Wei D. Antimicrobial Properties and Therapeutic Potential of Bioactive Compounds in *Nigella sativa*: A Review. Molecules, 29(20), 4914 (2024).
14. Mouwakeh A, Kincses A, Nové M, Mosolygó T, Mohácsi-Farkas C, Kiskó G, Spengler G. Nigella sativa essential oil and its bioactive compounds as resistance modifiers against Staphylococcus aureus. Phytother Res., 33(4), 1010-1018 (2019).
15. Dagtas S, Griffin RJ. *Nigella sativa* extract kills pre-malignant and malignant oral squamous cell carcinoma cells. J Herb Med., 29, 100473 (2021).
16. Peisker A, Raschke GF, Fahmy MD, Guentsch A, Roshanghias K, Hennings J, Schultze-Mosgau S. Salivary MMP-9 in the detection of oral squamous cell carcinoma. Med Oral Patol Oral Cir Bucal., 22(3), e270-275 (2017).
17. Kunigal S, Lakka SS, Joseph P, Estes N, Rao JS. Matrix metalloproteinase-9 inhibition down-regulates radiation-induced nuclear factor-kappa B activity leading to apoptosis in breast tumors. Clin Cancer Res., 14(11), 3617-26 (2008).
18. Smriti K, Ray M, Chatterjee T, Shenoy RP, Gadicherla S, Pentapati KC, Rustaqi N. Salivary MMP-9 as a Biomarker for the Diagnosis of Oral Potentially Malignant Disorders and Oral Squamous Cell Carcinoma. Asian Pac J Cancer Prev., 21(1), 233-238 (2020).
19. Hema Shree K, Gayathri R, Veeraraghavan VP, Ramani P, Ramadoss R, Yuwanati M. Gold nanoparticle enhanced TNFá antibody interface using saliva for predicting prognosis in OSCC. Arch Oral Biol., 173, 106196 (2025).
20. Rajeshkumar S, Parameswari RP, Jayapriya J, Tharani M, Ali H, Aljarba NH, Alkahtani S, Alarifi S. Apoptotic and Antioxidant Activity of Gold Nanoparticles Synthesized Using Marine Brown Seaweed: An In Vitro Study. Biomed Res Int., 2022, 5746761 (2022).
21. Kasabwala H, Ganapathy D, Shanmugam R. Green preparation of gold nano particles procured from neem and ginger plant extract to evaluate the antimicrobial activity against oral aerobic pathogens. Journal of Research in Medical and Dental Science, 9(6), 259-62 (2021).
22. Kim C, Kang MS, Raja IS, Joung YK, Han DW. Advancements in nanobiosensor technologies for in-vitro diagnostics to point of care testing. Heliyon, 30, 10(22) (2024).
23. Boccellino M, De Rosa A, Di Domenico M. An ELISA Test Able to Predict the Development of Oral Cancer: The Significance of the Interplay between Steroid Receptors and the EGF Receptor for Early Diagnosis. Diagnostics (Basel), 13(12), 2001 (2023).
24. Dagtas S, Griffin RJ. *Nigella sativa* extract kills pre-malignant and malignant oral squamous cell carcinoma cells. J Herb Med., 29, 100473 (2021).
25. Bashir MU, Qureshi HJ, Saleem T. Comparison of anti-inflammatory activity of nigella sativa and diclofenac sodium in albino rats. J Ayub Med Coll Abbottabad., 27(3), 523-6 (2015).
26. Kwan K, Han AY, Mukdad L, Barragan F, Selim O, Alhiyari Y, St John M. Anticancer effects of thymoquinone in head and neck squamous cell carcinoma: A scoping review. Laryngoscope Investig Otolaryngol., 8(4), 876-885 (2023).
27. Bashir MU, Qureshi HJ, Saleem T. Comparison of anti-inflammatory activity of nigella sativa and diclofenac sodium in albino rats. J Ayub Med Coll Abbottabad., 27(3), 523-6 (2015).
28. Malekipour MH, Shirani F, Moradi S, Taherkhani A. Cinnamic acid derivatives as potential matrix metalloproteinase-9 inhibitors: molecular docking and dynamics simulations. Genomics Inform., 21(1), e9 (2023).
29. Ahmad S, Abbasi HW, Shahid S, Gul S, Abbasi SW. Molecular docking, simulation and MM-PBSA studies of *nigella sativa* compounds: a computational quest to identify potential natural antiviral for COVID-19 treatment. J Biomol Struct Dyn., 39(12), 4225-4233 (2021).
30. Gimferrer M, Danés S, Andrada DM, Salvador P. Merging the Energy Decomposition Analysis with the Interacting Quantum Atoms Approach. J Chem Theory Comput., 19(12), 3469-3485 (2023).
31. Almajali B, Al-Jamal HAN, Taib WRW, Ismail I, Johan MF, Doolaanea AA, Ibrahim WN. Thymoquinone, as a Novel Therapeutic Candidate of Cancers. Pharmaceuticals (Basel), 14(4), 369 (2021).
32. Bs A, P A, As SG, A P, J VP. Analysis of differentially expressed genes in dysplastic oral keratinocyte cell line and their role in the development of HNSCC. J Stomatol Oral Maxillofac Surg., 125(4S), 101928 (2024).
33. Arumugam P, Jayaseelan VP. A novel m6A reader RBFOX2 expression is increased in oral squamous cell carcinoma and promotes tumorigenesis. Journal of Stomatology, Oral and Maxillofacial Surgery, 126(1), 102041 (2025).